View metadata, citation and similar papers at core.ac.uk

brought to you by CORE

provided by Exeley Inc.

exeley

Article | DOI: 10.21307/jofnem-2018-005

JOURNAL OF NEMATOLOGY

Issue 1 | Vol. 50

Postembryonic Ventral Nerve Cord Development and Gonad Migration in *Steinernema carpocapsae*

Hung Xuan Bui,[1,2,3] and Nathan E. Schroeder[1]*

[1]Department of Crop Sciences, University of Illinois at Urbana-Champaign, Urbana, IL, 61801.

[2]International Rice Research Institute, DAPO Box 7777, Metro Manila, Philippines.

[3]Department of Plant Protection, College of Agriculture and Applied Biology, Can Tho University, Can Tho, Vietnam.

*Email: nes@illinois.edu.

This article was edited by David Shapiro-Ilan.

Received for publication August 29, 2017.

Abstract

Steinernema carpocapsae is an entomopathogenic nematode widely studied for its properties as a biocontrol agent in insect pest management and as a model for understanding bacterial symbioses. Less attention has been given to the development of specific anatomical structures within *S. carpocapsae*. A better understanding of entomopathogenic nematode development and anatomy may lead to improved biocontrol efficacy. We recently demonstrated that the neuroanatomy of *S. carpocapsae* IJs differs from the dauer stage of *Caenorhabditis elegans*. Here, we used in vitro cultures of *S. carpocapsae* to examine the early development of the ventral nerve cord (VNC). Similar to *C. elegans, S. carpocapsae* hatches as a J1 with a VNC containing only a fraction of the neurons found in later developmental stages. During J1 development, *S. carpocapsae* adds additional cells to the VNC to establish the complete set of neurons. During our examination of the VNC, we also noted variable gonad arm development among *S. carpocapsae* individuals. Using synchronized in vitro cultures, we found that the gonad migration pattern in *S. carpocapsae* was distinct from both *C. elegans* and the Diplogaster nematode *Pristionchus pacificus*. The *S. carpocapsae* gonad arm migration was highly variable.

Key words

DAPI, DIC, distal tip cell, entomopathogenic nematode, preanal ganglion, retrovesicular ganglion, vulva.

Steinernema spp. are entomopathogenic nematodes used for the control of insect pests and for the study of bacterial symbiosis (Mandel, 2010; Lacey and Georgis, 2012). Although the general life cycle of *Steinernema* species is well established, their postembryonic development has received little attention. As part of a comparative study, we recently demonstrated that the ventral nerve cord (VNC) of the infective juvenile (IJ) stage of *Steinernema carpocapsae* and *Steinernema feltiae* differed substantially from the dauer stage of *Caenorhabditis elegans* (Han et al., 2016).

The VNC of *C. elegans* comprises a linear series of 57 motor neurons that synapse to most body wall muscles. The VNC is bound at the anterior end by the retrovesicular ganglion (RVG) and at the posterior end by the preanal ganglion (PAG), each of which contains additional motor neurons (Sulston, 1976; White et al., 1976). We previously found that IJs of both *S. carpocapsae* and *S. feltiae* contain approximately 20 more putative neurons in the VNC than *C. elegans* (Han et al., 2016).

The development of the VNC in *C. elegans* is well described. *C. elegans* hatches as a J1 with only 15 VNC neurons. During J1 development, a series of subventral precursor cells migrate into the VNC and divide to form the remainder of the VNC. By late J2,

© The Society of Nematologists 2018.

C. elegans hermaphrodites have completed VNC development (Sulston, 1976; Sulston and Horvitz, 1977). In our previous study, we found diversity in the timing of VNC development among select species (Han et al., 2016). However, the development of the VNC in *Steinernema* was not explored.

The initial objective of this study was to describe the development of the VNC in *S. carpocapase* during postembryonic development. However, during the course of our observations, we also noted divergence in gonad arm morphology between *C. elegans* and *S. carpocapsae*. The gonads of *C. elegans* hermaphrodites and males undergo stereotypical outgrowth that is under strict genetic control (Kimble and Hirsh, 1979; Antebi et al., 1997). To better illustrate the differences in gonad arm migration between *S. carpocapsae* and *C. elegans,* we conducted a time-series analysis of gonad development in *S. carpocapsae* grown on a *Xenorhabdus nematophila* bacterial culture. Our data suggest that although neurodevelopmental timing is conserved between *C. elegans* and *S. carpocapsae,* gonad arm migration has diverged between these species. Furthermore, we found substantial diversity in gonad arm migration patterns among *S. carpocapsae* adults.

Materials and methods

S. carpocapsae (a gift from A. Koppenhöfer, Rutgers University) were maintained on greater wax worm larvae *Galleria mellonella* (Carolina Biological Supply Company, Burlington, NC, USA) (Kaya and Stock, 1997). IJs were collected using the modified White trap method (Orozco et al., 2014). An in vitro culture of *S. carpocapsae* was established based on modification of previous methods (Volgyi et al., 1998). In summary, ten IJs were surface sterilized by rapid immersion in 95% ethanol. IJs were then immediately transferred to 20 µL of LB broth in a sterile Petri dish and cut open under a dissecting microscope with a sterile hypodermic needle to release the *X. nematophila* endosymbiotic bacteria. The LB broth containing bacteria was pipetted into 100 mL of LB broth and incubated overnight at 28°C on a shaker at 200 rpm. Overall, 100 µL of bacterial culture was aliquoted onto lipid agar (16 g nutrient broth, 5 g yeast extract, 5 g commercial vegetable oil, 15 g agar, 15 mM $NaPO_4$ buffer [pH7.0], 1 L H_2O) and incubated at 25°C in the dark for 24 to 48 h. Approximately 100 IJs were transferred to plates with a thick bacterial lawn and incubated at 25°C in the dark (Volgyi et al., 1998). After 3 to 4 days, IJs had recovered and developed to egg-laying adults. Eggs were transferred to fresh lipid agar plates with *X. nematophila* and incubated at 25°C in the dark. Nematodes were picked at specific time points after transferring eggs. Developmental stages were estimated based on the length and width of animals, the morphology of sexual structures, and a previously established developmental timeline in liquid culture (Hirao et al., 2010).

To examine the VNC of *S. carpocapsae*, specific developmental stages were collected from lipid agar plates and washed three times with phosphate buffered saline with 0.1% Triton X-100 (PBST) to remove excess *X. nematophila*. Nematodes were fixed in 1% formaldehyde on ice for one hour followed by methanol on ice for two minutes. Fixed nematodes were washed three times in PBST and then incubated in 0.2 to 0.5 µg/mL of 4′, 6-diamidino-2-phenylindole (DAPI, Life Technologies, Carlsbad, CA, USA) for 30 to 60 min (Duerr, 2006). Approximately 50 nematodes at each developmental stage were examined with fluorescence microscopy. Z-stack images were captured using a Zeiss Axiocam. VNC neuronal nuclei were identified by their small compact shape (Sulston, 1976; Han et al., 2016). The number of VNC neurons was counted from immediately posterior of the RVG to immediately anterior of the PAG (Han et al., 2016).

To examine gonad development, nematodes were picked onto microscope slides prepared with flattened agar pads made from 6.25% Noble agar in Ringer's solution (100 mM NaCl, 1.8 mM KCl, 2 mM $CaCl_2$, 1 mM $MgCl_2$, 5 mM HEPES pH 6.9) (Sulston, 1976; Ciche and Sternberg, 2007) and 10 mM levamisole and examined with differential interference contrast (DIC) optics on a Zeiss AxioImager microscope at 100x magnification at 5, 9, 25, 33, 40, 44, 54, 72 and 96 hr after introducing eggs on bacterial plates. At least 20 nematodes were examined at each time point. Z-stacks were captured with a Zeiss Axiocam.

The length and width of nematodes were measured by ImageJ. Multiple images were stitched using the ImageJ pairwise stitching plugin (Preibisch et al., 2009). Color overlays of stitched images were created in Photoshop.

Results and discussion

The in vitro development of *S. carpocapsae* on lipid agar proceeded at a similar rate as recently shown in monoxenic liquid culture (Hirao et al., 2010). Using this timeline, we examined the VNC in DAPI-stained animals at each developmental stage. The VNC of J1 *S. carpocapsae* contained 19 VNC neuronal-like nuclei, whereas J2 *S. carpocapsae* contained 69 VNC neuronal-like nuclei (Table 1 and Fig. 1). J3s increased in

Table 1. Ventral cord neurons of J1, J2, and J3 stage of *Steinernema carpocapsae*.

Stage	VNC neuron nuclei mean (range)	*n*
J1	19 (16-21)	50
J2	69 (50-76)	50
J3	76 (69-88)	46

size but showed only slightly more VNC nuclei than in J2s (Table 1). These data suggest that *S. carpocapsae* has a similar VNC developmental timeline as *C. elegans*. Owing to the issues with fixation in later developmental stages, we were not able to confidently quantify the number of nuclei in J4 and adult nematodes.

During the course of examining the VNC, we observed obvious differences in the morphology of the female gonad in *S. carpocapsae* compared with the well-characterized *C. elegans* gonad. To verify our observations, we examined 28 live adult females 72 hr after egg transfer (HET) with DIC microscopy. At this time point, the vulva was completely formed and the gonad had differentiated into a uterus, spermathecal-uterine complex, and ovaries (Zograf et al., 2008). However, with the exception of one nematode, 72 HET *S. carpocapsae* females did not contain fertilized embryos, which limited the transparency of older adult females.

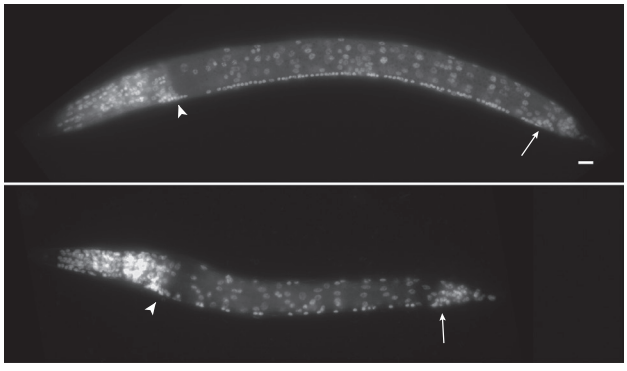

Figure 1: Lateral left view (anterior to left) fluorescent micrographs of J2 (top) and J1 (bottom) *Steinernema carpocapsae* following 4′, 6-diamidino-2-phenylindole (DAPI) staining. The ventral nerve cord (VNC) comprises a series of putative neurons extending from the retrovesicular ganglion (RVG) (arrowhead) to the preanal ganglion (PAG) (arrow) along the ventral edge of the animal. Between J1 and J2, there is a large increase in the number of VNC neuronal-like nuclei. Scale bar, 10 µm.

As observed in fixed animals, the gonad morphology of 72 HET *S. carpocapsae* females differed from *C. elegans* hermaphrodites. *C. elegans* hermaphrodites have a u-shaped gonad consisting of a proximal component that extends away from the mid-body along the ventral body wall followed by a sharp turn toward the dorsal body wall. During J4, the *C. elegans* hermaphrodite gonad completes migration by extending along the dorsal wall to the mid-body (Fig. 2A) (Kimble and Hirsh, 1979; Antebi et al., 1997).

The *S. carpocapsae* adult female gonad migration pattern has diverged substantially from *C. elegans* (Fig. 2B,C). The proximal *S. carpocapsae* female gonad, comprising the uterus, extended briefly along the ventral wall before wrapping around the intestine to the dorsal wall. The anterior arm typically wrapped around the right side of the intestine whereas the posterior arm wrapped around the left side of the intestine. Upon reaching the dorsal wall, the anterior arm extended anteriorly along the dorsal wall whereas the posterior arm extended posteriorly along the dorsal wall. After 640 to 1200 µm, the gonad made a U-turn and immediately extended back along the dorsal wall in the opposite direction (i.e. the anterior arm migrates posteriorly while the posterior arm migrates anteriorly). After migrating back to the mid-body, the gonad again extended toward the ventral wall. The distal end of the gonad was capped with a single cell that appears similar to the *C. elegans* distal tip cell (DTC). Owing to the larger body size and the presence of fertilized eggs, which obscured the optical clarity, we could not accurately trace the full gonad migration pattern in most 96 HET nematodes. However, a partial tracing of the gonad in several of the 96 HET females suggests a similar pattern as in 72 HET nematodes. The spermatheca-uterine complex (Zograf et al., 2008) of 96 HET females was located at the reflexed end of the gonad adjacent to the dorsal wall (Fig. 3). One difference between 72 and 96 HET nematodes is the greater extent of the ovary. In 72 HET nematodes, the DTC of each gonad arm typically only extends back to the mid-body, near the transverse plane of the vulva (Fig. 2). However, in 96 HET nematodes, the DTC of each gonad arm is found in the opposite field beyond the mid-body (i.e. the anterior gonad arm extends its ovary posterior of the vulva) (Fig. 3). Although our data suggest a standard gonad phenotype among

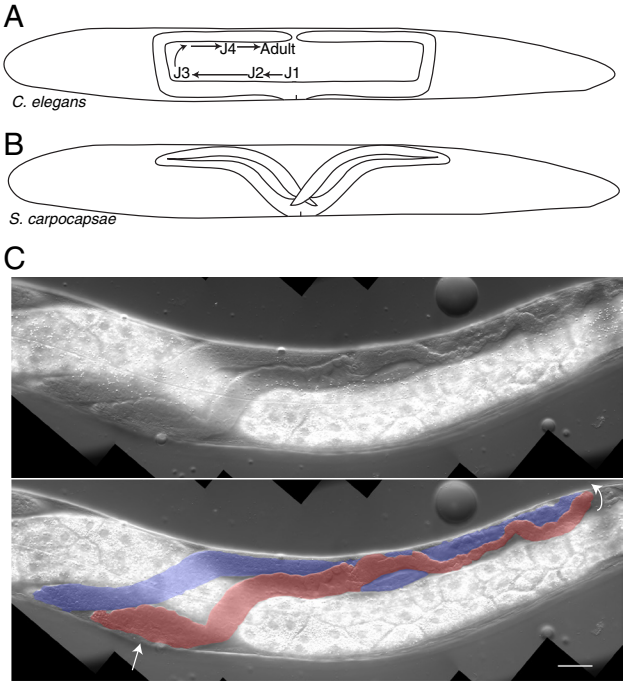

Figure 2: Cartoons of *Caenorhabditis elegans* (A) and *Steinernema carpocapsae* (B) gonads and lateral left view (anterior to left) micrograph of posterior *S. carpocapsae* gonad arm (C): differential interference contrast (DIC) alone (top); DIC color overlay (bottom). Unlike *C. elegans,* which undergoes stereotypical development to a 'U-shaped' gonad, the most common *S. carpocapsae* gonad shape does not include extensive migration along the ventral wall. As shown in the stitched DIC micrograph (C) (top) and with transparent color overlay (bottom), the gonad extends from the central region of the animal near the vulva (position indicated with straight arrow) and immediately extends to the dorsal side where it extends away from the mid-body. It eventually makes a u-turn (curved arrow) and then extends along the dorsal wall back to the mid-body where it then migrates back to the ventral wall. The posterior gonad arm typically wraps around the left side of the intestine, whereas the anterior arm typically wraps around the right side of the intestine. The proximal end of the gonad, including the uterus and spermathecal-uterine complex, is colored red. The distal end of the gonad following the turn includes the ovary and is colored blue. Scale bar, 50 µm.

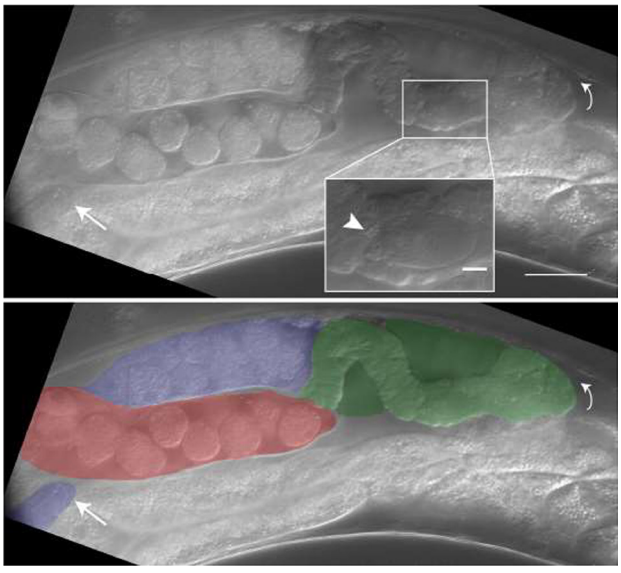

Figure 3: Lateral left view (anterior to left) differential interference contrast (DIC) micrograph (top) and with transparent color overlay (bottom) of a 96 HET female *Steinernema carpocapsae* gonad posterior arm. The gonad morphology at 96 HET is similar to that seen at 72 HET. However, by 96 HET, numerous fertilized embryos are seen in the uterus (red). The spermathecal-uterine complex (green) is located at the farthest point away from the mid-body and contains a single oocyte (inset) surrounded by numerous sperm (arrowhead). The ovary (blue) is much longer than in 72 HET females, frequently extending beyond the mid-body plane. In this image, the distal tip cell of the anterior gonad arm (arrow) extends into the posterior half of the female. Scale bars, 50 µm (main figure) 10 µm (inset).

S. carpocapsae females, we recorded substantial variability in the gonad migration pattern among 72 HET females (Fig. 4). Among females with atypical gonad migrations, the anterior and posterior arms were not always identical suggesting that the posterior and anterior arms can migrate independently.

We further characterized gonad development in *S. carpocapsae* by examining nematodes at earlier time points following egg transfer. Within 5 HET ($n=27$), J1s began to hatch. Similar to *C. elegans,* the gonad of newly hatched *S. carpocapsae* contained four nuclei with two central larger nuclei and two smaller cap nuclei that are likely homologous to the Z2,Z3 and Z1,Z4

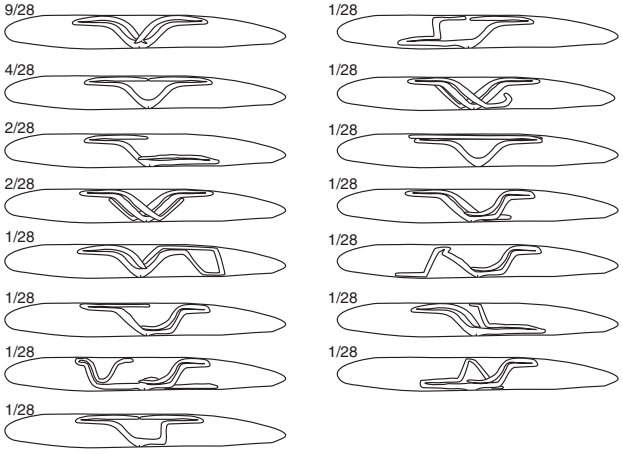

Figure 4: Cartoon depicting the variability in the gonad migration pattern among 72 HET *Steinernema carpocapsae* females that deviate from the most common phenotype seen in figure 2C. Numbers indicate the ratio of the particular gonad phenotype among the 28 females whose gonads were fully traced.

cells in *C. elegans,* respectively (Fig. 5A) (Kimble and Hirsh, 1979). Similar to *C. elegans,* this early gonad crossed the ventral midline (Kimble and Hirsh, 1979). By 25 HET ($n=20$), the number of nuclei in the J2 gonad had noticeably increased and elongated along the ventral body wall (Fig. 5B). At 33 HET ($n=24$), the gonad reached the dorsal surface (Fig. 5C). Between 44 HET ($n=20$) and 54 HET ($n=40$), we observed an expansion of the J4 gonad along the dorsal surface (Figure 5D,E). Interestingly, we did not observe the distal end of the gonad ever pointing away from the mid-body as would be expected based on our observations at 72 HET. Rather than a continual "pulling" of the gonad from the DTC, as seen in *C. elegans,* our observations may imply that outgrowth of the gonad can occur from more proximal locations. To confirm this observation, we attempted to perform time-lapse imaging of *S. carpocapsae* as previously demonstrated for *C. elegans.* However, all of our attempts at live time-lapse imaging on a microscope slide were unsuccessful.

The gonad morphology of most *S. carpocapsae* males is very similar to that seen in *Pristionchus pacificus* and *C. elegans* (Kimble and Hirsh, 1979; Hubbard and Greenstein, 2005; Rudel et al., 2005). The male gonad extends anteriorly from the mid-body along the ventral wall and then turns towards the dorsal wall. Upon reaching the dorsal wall, the

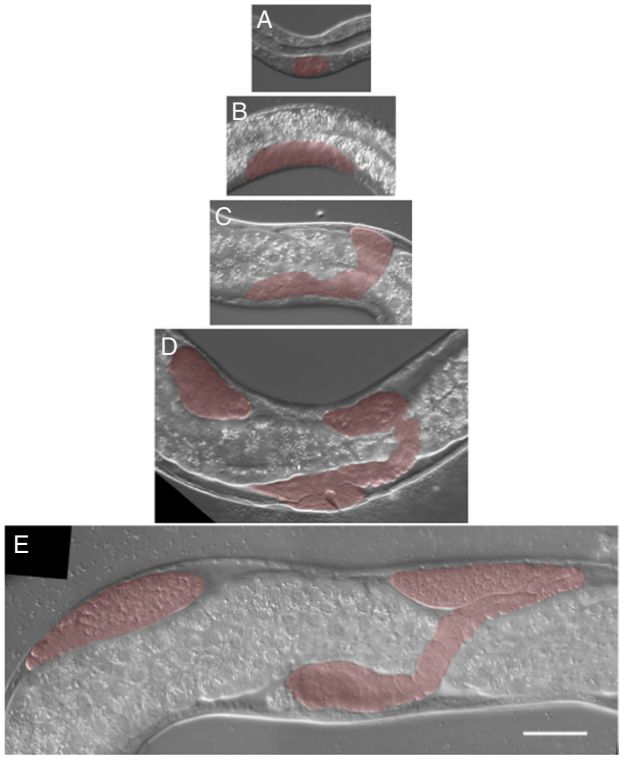

Figure 5: Lateral left views (anterior to left) of female gonad (red overlay) development in *Steinernema carpocapsae* at various time points. The gonad of newly hatched *S. carpocapsae* (A) contained four nuclei with two central larger nuclei and two smaller cap nuclei. By 25 HET (B), the number of nuclei in the gonad noticeably increased and began elongating along the ventral body wall. At 33 HET (C), the gonad extended toward the dorsal surface. Between 44 HET (D) and 54 HET (E), we observed an expansion of the gonad along the dorsal surface. Note that the anterior arm typically wraps around the right side of the intestine and is out of frame at this focal plane, whereas the posterior arm wraps around the left side. Scale bar, 50 µm.

male gonad extends posteriorly toward the spicules (Fig. 6A). Similar to the variability in females, we observed a variable male gonad migration pattern in 30% ($n=51$) of males wherein the gonad never migrates to the dorsal side (Fig. 6B).

The postembryonic development of most nematodes has not been studied in detail. The development of endoparasitic nematode species is

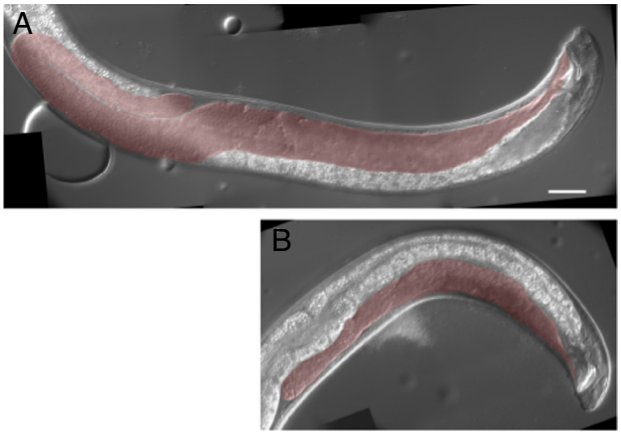

Figure 6: Lateral right (A) and left (B) views of gonad (red) morphology in male *Steinernema carpocapsae* at 72 HET. In most males (A), the gonad migration pattern is similar to *C. elegans.* However, 30% of males examined have a gonad that never extends away from the ventral wall (B). Scale bar, 50 µm.

particularly challenging to record within their host. However, our in vitro data suggest that although *S. carpocapsae* utilizes similar timing for the development of its nervous system, the migration of the gonad has diverged from the nematodes *C. elegans* and *P. pacificus.* Gonad arm migration in *C. elegans* is under strict genetic control. It will be interesting to determine if homologous genes function in *S. carpocapsae* to regulate gonad arm migration.

References

Antebi, A., Norris, C.R., Hedgecock, E.M., and Garriga, G. 1997. Cell and growth cone migrations, in Riddle, D.L. (Ed.), *C. elegans* II, Cold Spring Harbor Press, Cold Spring Harbor, NY, pp. 583–609.

Ciche, T.A., and Sternberg, P.W. 2007. Postembryonic RNAi in *Heterorhabditis bacteriophora*: a nematode insect parasite and host for insect pathogenic symbionts. *BMC Developmental Biology* 7(1): 101.

Duerr, J.S. 2006. Immunohistochemistry, (June 19, 2006). The *C. elegans* Research Community, ed. WormBook. Doi/10.1895/wormbook.1.105.1, http://www.wormbook.org.

Han, Z., Boas, S., and Schroeder, N.E. 2016. Unexpected variation in neuroanatomy among diverse nematode species. *Frontiers in Neuroanatomy* 9: 162.

Hirao, A., Ehlers, R.U., and Strauch, O. 2010. Life cycle and population development of the entomopathogenic nematodes *Steinernema carpocapsae* and *S. feltiae* (Nematoda, Rhabditida) in monoxenic liquid culture. *Nematology* 12(2): 201–10.

Hubbard, E.J.A., and Greenstein, D. 2005. Introduction to the germ line, (September 1, 2005). The *C. elegans* Research Community, ed. WormBook. doi/10.1895/wormbook.1.18.1, http://www.wormbook.org.

Kaya, H.K., and Stock, S.P. 1997. Techniques in insect nematology, in Lacey, L.A. (Eds), *Manual of Techniques in Insect Pathology*, Academic Press, London.

Kimble, J., and Hirsh, D. 1979. The postembryonic cell lineages of the hermaphrodite and male gonads in *Caenorhabditis elegans*. *Developmental Biology* 70(2): 396–417.

Lacey, L.A., and Georgis, R. 2012. Entomopathogenic nematodes for control of insect pests above and below ground with comments on commercial production. *Journal of Nematology* 44(2): 218–25.

Mandel, M.J. 2010. Models and approaches to dissect host–symbiont specificity. *Trends in Microbiology* 18(11): 504–11.

Orozco, R.A., Lee, M.M., and Stock, S.P. 2014. Soil sampling and isolation of entomopathogenic nematodes (Steinernematidae, Heterorhabditidae). *Journal of Visualized Experiments* 89: 1–8, doi: 10.3791/52083.

Preibisch, S., Saalfeld, S., and Tomancak, P. 2009. Globally optimal stitching of tiled 3D microscopic image acquisitions. *Bioinformatics* 25(11): 1463–5.

Rudel, D., Riebesell, M., and Sommer, R.J. 2005. Gonadogenesis in *Pristionchus pacificus* and organ evolution: development, adult morphology and cell–cell interactions in the hermaphrodite gonad. *Developmental Biology* 277(1): 200–21.

Sulston, J.E. 1976. Post-embryonic development in the ventral cord of *Caenorhabditis elegans*. *Philosophical Transactions of the Royal Society of London B: Biological Sciences* 275(938): 287–97.

Sulston, J.E., and Horvitz, H.R. 1977. Post-embryonic cell lineages of the nematode, *Caenorhabditis* elegans. *Developmental Biology* 56(1): 110–56.

Volgyi, A., Fodor, A., Szentirmai, A., and Forst, S. 1998. Phase variation in *Xenorhabdus nematophilus*. *Applied and Environmental Microbiology* 64(4): 1188–93.

White, J.G., Southgate, E., Thomson, J.N., and Brenner, S. 1976. The structure of the ventral nerve cord of *Caenorhabditis elegans*. *Philosophical Transactions of the Royal Society of London B: Biological Sciences* 275(938): 327–48.

Zograf, J.K., Bert, W., and Borgonie, G. 2008. The structure of the female reproductive system of nematodes from the genus Steinernema (Rhabditida: Steinernematidae). *Nematology* 10(6): 883–96.